

Molecular Modeling of Ruthenium Alkylidene Mediated Olefin Metathesis Reactions. DFT Study of Reaction Pathways

Serguei Fomine,* Sergio Martinez Vargas, and Mikhail A. Tlenkopatchev

Instituto de Investigaciones en Materiales, Universidad Nacional Autónoma de México, Apartado Postal 70-360, CU, Coyoacán, México DF 04510, México

Received July 22, 2002

Three possible reaction pathways have been studied for the $\text{Cl}_2(\text{PMe}_3)_2\text{Ru}=\text{CH}_2$ and $\text{Cl}_2(\text{PCy}_3)_2\text{Ru}=\text{CH}_2$ (Cy = cyclohexyl) mediated metathesis reaction of propylene by quantum-mechanical DFT calculations. It was found that in all cases the metathesis reaction proceeds via dissociative substitution of a phosphine ligand with propylene, giving a monophosphine complex. This tendency increases with ligand volume, and in the case of smaller PMe_3 groups it is the entropy contribution to the reaction energetics that causes the monophosphine complex to participate in the metathesis reaction, according to the modeling data.

Introduction

Metal carbene (alkylidene) complexes play a very important role as intermediates in homogeneous catalysis reactions such as olefin metathesis, olefin and acetylene polymerization, and cyclopropanation.¹ In particular, olefin metathesis has a variety of applications. Thus, ring-opening metathesis polymerization, acyclic diene metathesis polymerization, cross-metathesis, and ring-closing metathesis are widely used in organic and polymer chemistry. Many reviews devoted to the metathesis reaction have been published² to date. It is generally accepted that olefin metathesis occurs via the so-called metal alkylidene (carbene) chain mechanism first proposed by Herrison and Chauvin.³ This reaction proceeds via a metallacyclobutane intermediate to form a new metal carbene and a new olefin (Figure 1). The proposed mechanism stimulated the development of new metal alkylidene and metallacyclobutane single-component homogeneous catalysts.^{4–8} Thus, a number of new well-defined ruthenium alkylidene catalysts have been synthesized.⁹ Ruthenium alkylidene catalysts have attracted much attention due to their activity, stability, and selectivity. These catalysts allow

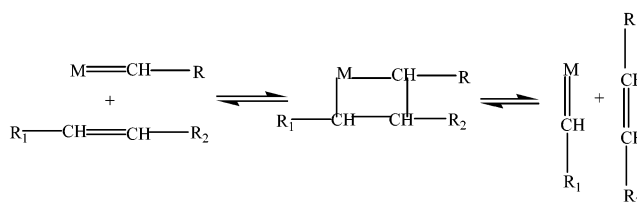


Figure 1. General mechanism of the olefin metathesis.

the synthesis of cyclic and linear molecules with trisubstituted unsaturations and diverse functionalities under mild conditions.^{10,11}

The mechanism of ruthenium alkylidene catalyzed olefin metathesis has recently been the subject of intense investigations.^{12,13} These results clearly indicate that the key step in the catalytic cycle of the metathesis reaction is initial phosphine ligand substitution by an olefin substrate. The substitution may proceed via an associative or a dissociative pathway.¹⁴ It was postulated that for the ruthenium complexes with the general formula $\text{L}(\text{PR}_3)(\text{X})_2\text{Ru}=\text{CHR}^1$ ($\text{R} = \text{Cy}, \text{Cp}, \text{Ph}, \text{Bn}$; $\text{X} = \text{Cl}, \text{Br}, \text{I}$; $\text{L} = \text{N-heterocyclic carbene ligand, NHC}$) the initiation occurs by dissociative substitution of a phosphine ligand (PR_3) with olefin substrate.¹⁴

(1) For general reviews, see: (a) Ivin, K. J.; Mol, J. C. *Olefin Metathesis and Metathesis Polymerization*; Academic Press: San Diego, CA, 1997. (b) Dörwald, F. Z. *Metal Carbenes in Organic Synthesis*; Wiley-VCH: Weinheim, Germany, 1999. (c) Herrmann, W. A. *Angew. Chem., Int. Ed.* **2002**, *41*, 1290.

(2) For recent reviews, see: (a) Grubbs, R. H.; Chang, S. *Tetrahedron* **1998**, *54*, 4413. (b) Wright, D. L. *Curr. Org. Chem.* **1999**, *3*, 211–240. (c) Buchmeiser, M. R. *Chem. Rev.* **2000**, *100*, 1565. (d) Fürstner, A. *Angew. Chem., Int. Ed.* **2000**, *39*, 3012.

(3) Herisson, J. L.; Chauvin, Y. *Makromol. Chem.* **1971**, *141*, 161.

(4) (a) Katz, T. J.; Lee, S. J.; Acton, N. *Tetrahedron Lett.* **1976**, *47*, 4247–4250. (b) Katz, T. J.; Sivavec, T. M. *J. Am. Chem. Soc.* **1985**, *107*, 737.

(5) Quignard, F.; Leconte, M.; Basset, J.-M. *J. Chem. Soc., Chem. Commun.* **1985**, 1816.

(6) (a) Kress, J.; Osborn, J. A.; Greene, R. M. E.; Ivin, K. J.; Rooney, J. J. *J. Am. Chem. Soc.* **1987**, *109*, 899. (b) Kress, J.; Aguero, A.; Osborn, J. A. *J. Mol. Catal.* **1986**, *36*, 1.

(7) Wallace, K. C.; Liu, A. H.; Dewan, J. C.; Schrock, R. R. *J. Am. Chem. Soc.* **1988**, *110*, 4964–4977.

(8) For reviews, see: (a) Schrock, R. R. *Acc. Chem. Res.* **1990**, *23*, 158. (b) Schrock, R. R. *Tetrahedron* **1999**, *55*, 8141.

(9) (a) Nguyen, S. T.; Johnson, L. K.; Grubbs, R. H.; Ziller, J. W. *J. Am. Chem. Soc.* **1992**, *114*, 3974–3975. (b) Wu, Z.; Benedicto, A. D.; Grubbs, R. H. *Macromolecules* **1993**, *26*, 4975. (c) Nguyen, S. T.; Grubbs, R. H.; Ziller, J. W. *J. Am. Chem. Soc.* **1993**, *115*, 9858. (d) Hilmyer, M. A.; Laredo, W. R.; Grubbs, R. H. *Macromolecules* **1995**, *28*, 6311.

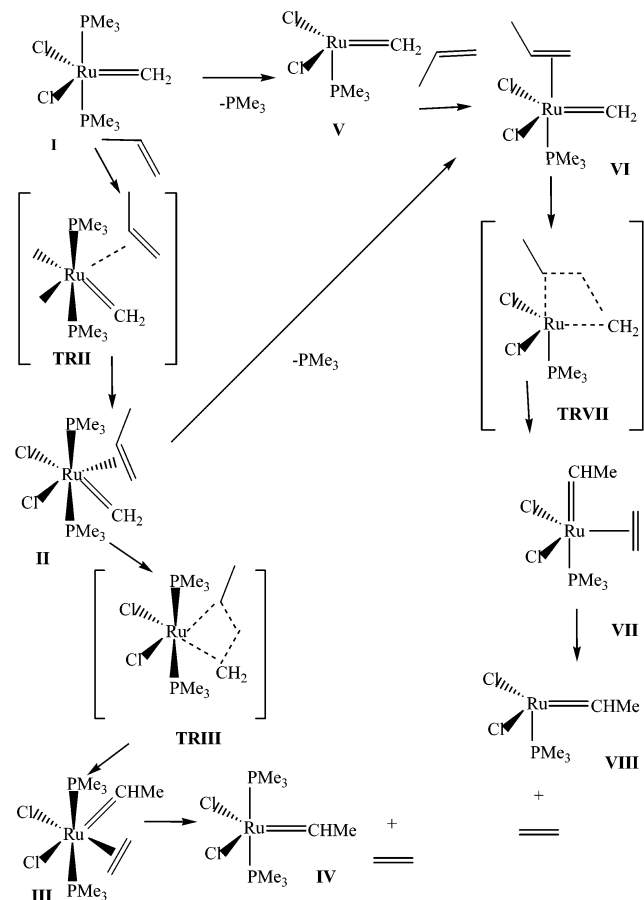
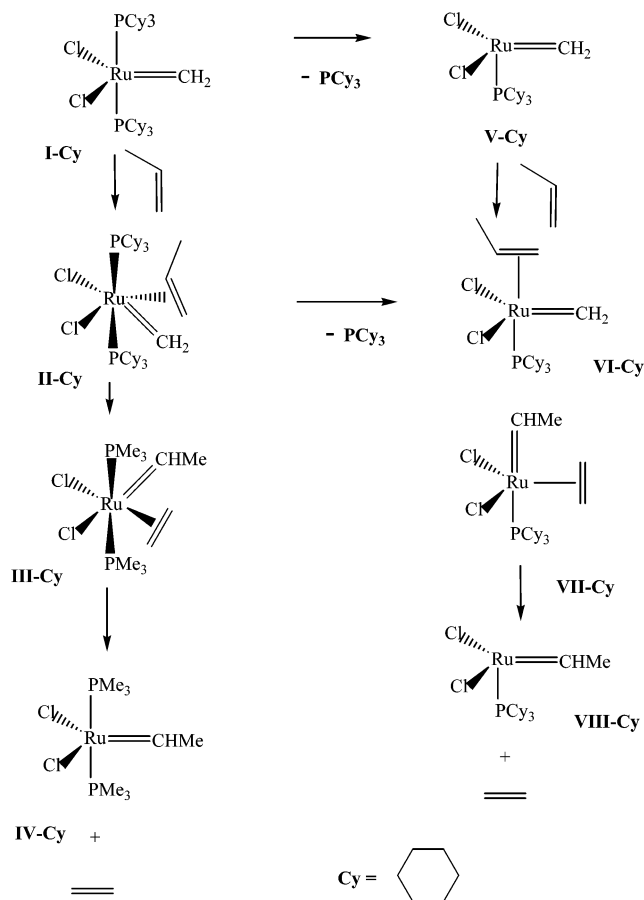
(10) Craig, S. W.; Manzer, J. A.; Coughlin, E. B. *Macromolecules* **2001**, *34*, 7929.

(11) (a) Miller, S. J.; Blackwell, H. E.; Grubbs, R. H. *J. Am. Chem. Soc.* **1996**, *118*, 9606. (b) Ulman, M.; Belderrain, T. R.; Grubbs, R. H. *Tetrahedron Lett.* **2000**, *41*, 4689.

(12) (a) Dias, E. L.; Nguyen, S. T.; Grubbs, R. H. *J. Am. Chem. Soc.* **1997**, *119*, 3887. (b) Ulman, M.; Grubbs, R. H. *Organometallics* **1998**, *17*, 2484. (c) Sanford, M. S.; Ulman, M.; Grubbs, R. H. *J. Am. Chem. Soc.* **2001**, *123*, 749.

(13) (a) Hinderling, C.; Adlhart, C.; Chen, P. *Angew. Chem., Int. Ed.* **1998**, *37*, 2685. (b) Adlhart, C.; Hinderling, C.; Baumann, H.; Chen, P. *J. Am. Chem. Soc.* **2000**, *122*, 8204. (c) Adlhart, C.; Chen, P. *Helv. Chim. Acta* **2000**, *83*, 2192.

(14) Sanford, M. S.; Love, J. A.; Grubbs, R. H. *J. Am. Chem. Soc.* **2001**, *123*, 6543.

Scheme 1. Reaction Paths of the Propylene Metathesis Reaction Mediated by PMe_3 -Containing Ru Complexes**Scheme 2. Reaction Paths of the Propylene Metathesis Reaction Mediated by PCy_3 -Containing Ru Complexes**

Although the olefin metathesis reaction is one of the most studied in organometallic chemistry, there have been few reports dealing with modeling of this metal-catalyzed reaction using quantum chemistry tools. Thus, Rappe¹⁵ reported the modeling of a metathesis reaction catalyzed by high-valent group VI metals. Density functional and second-order Møller–Plesset theory were used to model $\text{W}(0)$ carbene mediated propylene metathesis.¹⁶ In recent quantum molecular dynamics studies¹⁷ performed on the simple model $\text{Cl}_2(\text{PH}_3)_2\text{Ru}=\text{CH}_2/\text{C}_2\text{H}_4$, the conclusion has been reached that the reason the monophosphine complex is more active in metathesis reactions compared to diphosphine complex is that there is more space available on the Ru center of monophosphine complex. The Ru catalyst activity, however, depends so much on the phosphine structure¹⁴ that the representation of a phosphine ligand by such a simple molecule as PH_3 might be qualitatively wrong. Novel computational studies of ruthenium-catalyzed olefin metathesis reactions have recently been published where first generation of Grubbs-type $(\text{PCy}_3)_2\text{Cl}_2\text{Ru}=\text{CHPh}$ (pre)catalyst, as well as in the heteroleptic (pre)catalytic systems. It was found that in agreement with experiment PCy_3 coordinates more strongly

to Ru in the heteroleptic (pre)catalysts than in the Grubbs-type (pre)catalyst. Moreover, ethene coordination and insertion into the Ru–alkylidene bond in the above-mentioned systems, as well as in the Hofmann type catalytic system with a cis-coordinated phosphane ligand, have been studied.¹⁸

The goal of this paper is to carry out a computational study of Ru mediated propylene metathesis reaction mechanisms using the more realistic complexes $\text{Cl}_2(\text{PMe}_3)_2\text{Ru}=\text{CH}_2$ (**I**) (Scheme 1) and especially $\text{Cl}_2(\text{PCy}_3)_2\text{Ru}=\text{CH}_2$ (**ICy**) (Scheme 2) and fast Jaguar code¹⁹ allowing the modeling of large organometallic complexes at high theoretical levels and low computational costs.

Computational Details

All calculations were carried out with the program Jaguar, version 4.1.¹⁹ The geometry optimizations were run at the B3LYP/LACVP** level of theory.^{20–23} The LACVP basis set uses the standard 6-31G** basis set for valence electrons and the outermost set of core electrons of third row and heavier elements and the LAC pseudopotential²⁴ for inner core electrons. The elements of the first and second rows use the

(15) Reppe, A. K.; Goddard, W. *J. Am. Chem. Soc.* **1982**, *104*, 448.

(16) Tlenkopatchev, M.; Fomine, S. *J. Organomet. Chem.* **2001**, *630*, 157.

(17) (a) Aagaard, O. M.; Meier, R. J.; Buda, F. *J. Am. Chem. Soc.* **1998**, *120*, 7174. (b) Meier, R. J.; Aagaard, O. M.; Buda, F. *J. Mol. Catal.* **2000**, *160*, 189.

(18) Cavallo, L. *J. Am. Chem. Soc.* **2002**, *124*, 8965.

(19) Jaguar 4.1, Schrodinger, Inc., Portland, OR, 2000.

(20) Slater, J. C. *Quantum Theory of Molecules and Solids*; McGraw-Hill: New York, 1974; vol. 4.

(21) Vosko, S. H.; Wilk, L.; Nusair, M. *Can. J. Phys.* **1980**, *58*, 1200.

(22) Becke, A. D. *Phys. Rev.* **1988**, *38*, 3098.

(23) Lee, C.; Yang, W.; Parr, R. G. *Phys. Rev. B* **1988**, *37*, 785.

Table 1. Free (at 298.15 K), Total Electronic, and Solvation Energies (in hartrees) of Studied Molecules at the B3LYP/LACVP//B3LYP/LACVP** Level of Theory**

molecule	<i>G</i>	<i>E</i>	<i>E</i> _{solv}	molecule	<i>G</i>	<i>E</i>	<i>E</i> _{solv}
I	-1 975.710 062	-1 975.919 302	-0.018 064	VII	-1 632.524 082	-1 632.703 043	-0.012 914
propylene	-117.855 907	-117.910 727	-0.001 843	VIII	-1 553.969 796	-1 554.099 197	-0.017 476
TRII	-2 093.533 888	-2 093.817 549	-0.014 002	I-Cy		-3 148.093 192	-0.009 664
II	-2 093.536 644	-2093.825 883	-0.018 392	II-Cy		-3 265.958 144	-0.008 954
TRIII	-2 093.524 740	-2 093.814 457	-0.019 342	V-Cy		-2 100.863 518	-0.013 610
III	-2 093.543152	-2 093.832 550	-0.020 195	VI-Cy		-2 218.782 432	-0.007 653
IV	-2 015.010 926	-2 015.244 867	-0.012 544	PCy ₃		-1 047.191 79	-0.002 255
ethylene	-78.561 711	-78.591 989	-0.001 787	III-Cy		-3 265.966 938	-0.011557
PMe ₃	-461.023 818	-461.107 482	-0.003 582	IV-Cy		-3 187.403 890	-0.009 153
V	-1 514.672 011	-1 514.774 798	-0.017 077	VII-Cy		-2 218.785 064	-0.013 464
VI	-1 632.522 324	-1 632.702 401	-0.012 666	VIII-Cy		-2 140.180 578	-0.013 955
TRVII	-1 632.507 305	-1 632.688 657	-0.017 599				

Table 2. Reaction and Activation Energies (in kcal/mol; ΔE , E_a and ΔG , G^\ddagger at 298.15 K) Calculated at the B3LYP/LACVP//B3LYP/LACVP** Level of Theory**

reacn	gas phase				soln			
	ΔE	E_a	ΔG	G^\ddagger	$\Delta E + \Delta E_s$	$E_a + \Delta E_s$	$\Delta G + \Delta E_s$	$G^\ddagger + \Delta E_s$
I + propylene → II	2.6	7.8	18.1	20.1	3.6	11.5	19.1	23.8
II → III	-4.2	7.2	-3.8	7.8	-5.3	6.6	-4.9	7.2
III → IV + ethylene	-2.7		-18.5		-1.6		-17.4	
I → V + PMe ₃	23.2		8.9		21.6		7.3	
V + propylene → VI	-10.6		3.5		-6.7		7.4	
VI → VII	-0.4	8.6	-0.9	9.4	-0.4	5.5	-0.9	6.3
VII → VIII + ethylene	7.4		-4.9		4.0		-8.3	
II → VI + PMe ₃	10.0		-5.7		11.3		-4.4	
I-Cy + propylene → II-Cy	30.8				32.5			
II-Cy → III-Cy	-5.5				-7.1			
I-Cy → V-Cy + PCy ₃	23.7				19.8			
V-Cy + propylene → VI-Cy	-3.1				1.9			
II-Cy + PCy ₃ → VI-Cy	-10.1				-10.7			
VI-Cy → VII-Cy	-1.7				-5.3			
III-Cy → IV-Cy + ethylene	-18.2				-17.8			
VII-Cy → VIII-Cy + ethylene	7.9				6.5			

standard 6-31G** basis set. All structures except Cy-containing ones were characterized by frequency calculations to ensure that a transition state (one imaginary mode) or a minimum (zero imaginary modes) is located and to calculate free energies (*G*). The Poisson–Boltzmann solver^{25,26} implemented in Jaguar, version 4.1, was used to calculate the solvation effects on the studied molecules in chlorobenzene at the B3LYP/LACVP** level of theory. In other words, the structures have not been reoptimized in the presence of solvent, since previously it has been shown that reoptimization has a very limited effect on the computed energies.^{27–31} The applicability of the selected theoretical model was tested by comparison of bond lengths and angles of synthesized [Cl₂(PCy₃)₂-Ru=CHR] alkylidene complexes where Cy = cyclohexyl and R = tolyl³² with the model complex [Cl₂(PMe₃)₂Ru=CH₂] optimized at the B3LYP/LACVP** level. The agreement between experimental and calculated Ru–Cl, Ru–P, and Ru–C bond lengths was very reasonable. The maximum deviation from experiment was observed for Ru–Cl bond distances (0.04 Å longer). For Ru–P and Ru–C distances the

errors were within 0.02 Å. The bond angles Cl–Ru–Cl and P–Ru–P were reproduced very well by the adopted model. The deviations did not exceed 1°.

Results and Discussion

Scheme 1 shows possible reaction pathways for the model complex Cl₂(PMe₃)₂Ru=CH₂. One of the possibilities is the formation of the propylene complex **II** without loss of the PMe₃ molecule. On the other hand, complex **II** can either lose a PMe₃ molecule, giving the propylene complex **VI**, or undergo a metathesis reaction, forming ethylene complex **III**. In case of complex **VI** formation the metathesis reaction occurs, giving complex **VII** followed by its dissociation to monophosphine complex **VIII** and ethylene, while the dissociation of intermediate **III** results in formation of ethylene and diphosphine complex **IV**. Another reaction pathway involves complex **I**–**V** transformation, where complex **I** loses a PMe₃ molecule followed by formation of the propylene complex **VI**. Complex **VI** is transformed into ethylene complex **VII** via a metathesis reaction, giving monophosphine complex **VIII** and an ethylene molecule as final products of the metathesis reaction. Thus, three different metathesis reaction pathways are considered. The first pathway describes a process involving diphosphine complexes (**I**–**II**–**III**–**IV**); the second and third pathways (**I**–**II**–**VI**–**VII**–**VIII** and **I**–**V**–**VI**–**VII**–**VIII**) describe the propylene metathesis catalyzed by the monophosphine complex. Table 1, Table 2 and Figure 2 show reaction energetics for different reaction pathways. The first conclusion that can be made is that solvation effects do not change the qualitative picture of reaction

(24) Hay, P. J.; Wadt, W. R. *J. Chem. Phys.* **1985**, *82*, 270.

(25) Tannor, D. J.; Marten, B.; Murphy, R.; Friesner, R. A.; Sitkoff, D.; Nicholls, A.; Ringnalda, M.; Goddard, W. A., III; Honig, B. *J. Am. Chem. Soc.* **1994**, *116*, 11875.

(26) Marten, B.; Kim, K.; Cortis, C.; Friesner, R. A.; Murphy, R. B.; Ringnalda, M. N.; Sitkoff, D.; Honig, B. *J. Phys. Chem.* **1996**, *100*, 11775.

(27) Barone, V.; Cossi, M.; Tomasi, J. *J. Chem. Phys.* **1997**, *107*, 3210.

(28) Pomeli, C. S.; Tomasi, J.; Sola, M. *Organometallics* **1998**, *17*, 3164.

(29) Caselli, I.; Ferretti, A. *J. Chem. Phys.* **1998**, *109*, 8583.

(30) Creve, S.; Oevering, H.; Coussens, B. B. *Organometallics* **1999**, *18*, 1907.

(31) Bernardi, F.; Bottoni, A.; Miscone, G. P. *Organometallics* **1998**, *17*, 16.

(32) Schwab, P.; France, M. B.; Ziller, J. W.; Grubbs, R. H. *Angew. Chem., Int. Ed. Engl.* **1995**, *34*, 2039.

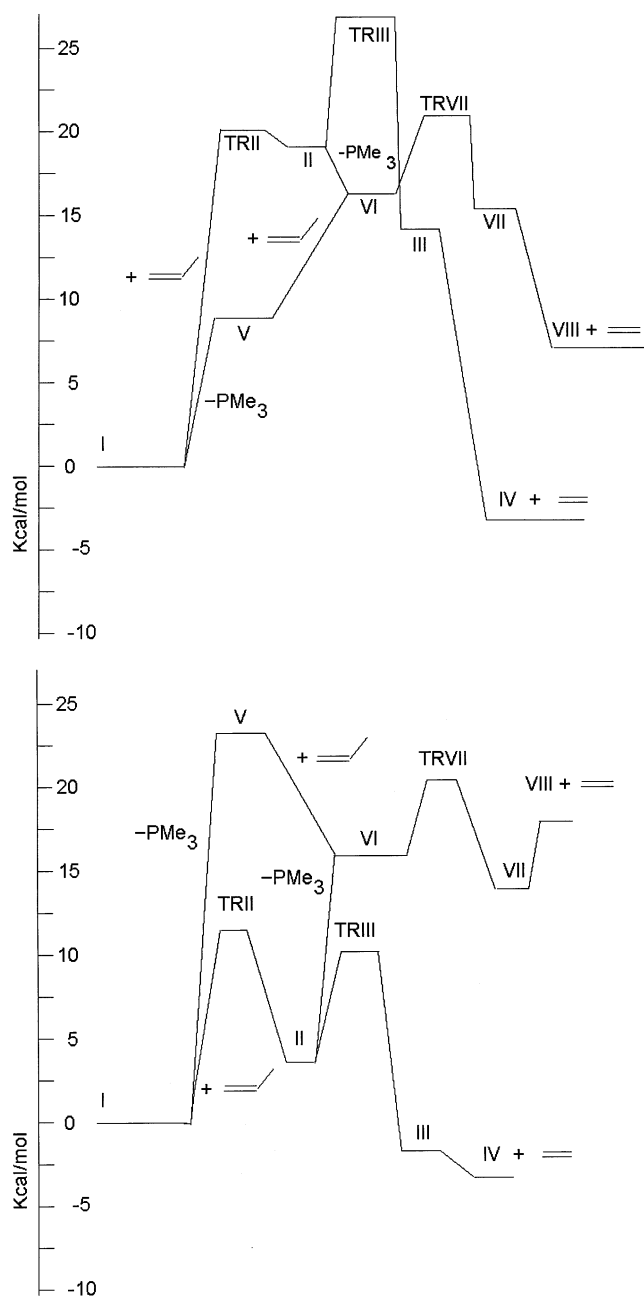


Figure 2. (a, top) Free energy profile for the propylene metathesis reaction mediated by PMe_3 containing Ru complexes. (b, bottom) Total electronic energy profile for the propylene metathesis reaction mediated by PMe_3 -containing Ru complexes.

energetics. In most cases the difference between the gas phase and solution is within 2 kcal/mol and in any case is within 4 kcal/mol. When considering first the reaction pathway for the PMe_3 ligand, one can see that the formation of propylene complex **II** is unfavorable, showing free activation energies of 20.1 and 23.8 kcal/mol in the gas phase and solution, respectively. A perceptible activation energy and positive free energy of this process are due to unfavorable entropy factors and steric hindrances caused by propylene molecule complexation. Thus, Ru–P bond distances increase from 2.41 Å in **I** to 2.46 and 2.44 Å in **II**. Moreover, one of the Ru–Cl bond distances also increases from 2.46 Å in **I** to 2.49 and 2.61 Å in **II** (Figure 3). Once complex **II** is formed, the metathesis takes place, forming the secondary

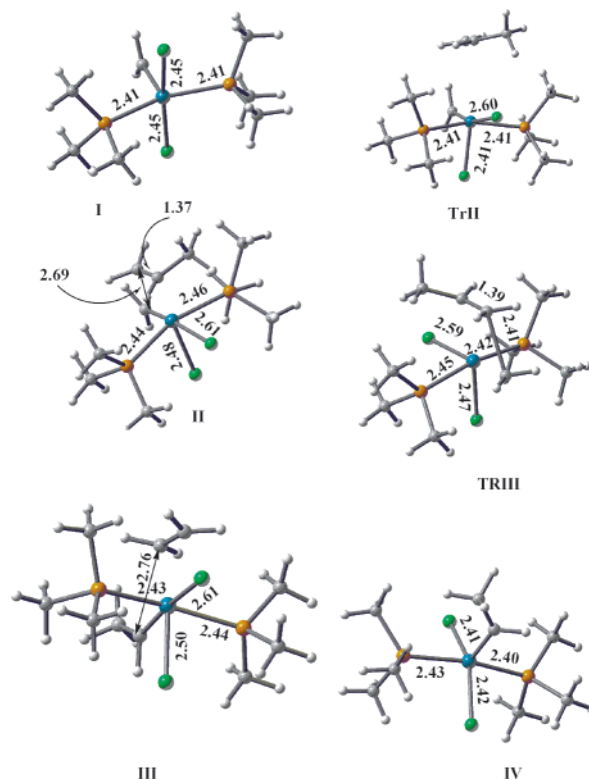


Figure 3. Equilibrium and transition state geometries of PMe_3 -containing Ru diphosphine complexes participating in the propylene metathesis reaction.

carbene–ethylene complex **III**. This reaction is characterized by a negative ΔG value, reflecting the higher stability of a secondary carbene compared to a primary one,¹⁶ and shows a low free activation energy (7.8 kcal/mol in the gas phase and 7.2 kcal/mol in solution). As can be seen from Figure 3 (comparing structures **II** and transition state **TRIII**), the carbene needs to rotate for metathesis to occur in accordance with the metathesis mechanism proposed by Grubbs,¹² since the carbene methylene is perpendicular to the propylene plane in complex **II** and parallel in the transition state **TRIII**. According to calculations the decomplexation of complex **III** is characterized by a negative free energy due to favorable entropy factors and steric hindrances caused by the olefin molecule in diphosphine complexes.

The first step of the second metathesis reaction pathway involves the dissociation of the Ru–P bond in complex **II** to produce the monophosphine complex **VI**. This reaction is characterized by negative ΔG values (–5.7 and –4.4 kcal/mol in the gas phase and in solution, respectively), comparing favorably with the free activation energy of the **II**–**III** process (about 7 kcal/mol). The relaxed potential energy search carried out for complex **II** Ru–P bond dissociation at the B3LYP/LACVP** level does not reveal, however, any perceptible activation energy for this process. Therefore, the **II**–**VI** process should be the predominant transformation for complex **II** once it has been formed. Thus, the first reaction pathway seems to be unfavorable compared to the second one.

The third reaction pathway involves the dissociation of biphosphine complex **I** first to form the monophosphine complex **V** and PMe_3 . Thus, free energies for this reaction are only 8.9 and 7.3 kcal/mol in the gas phase

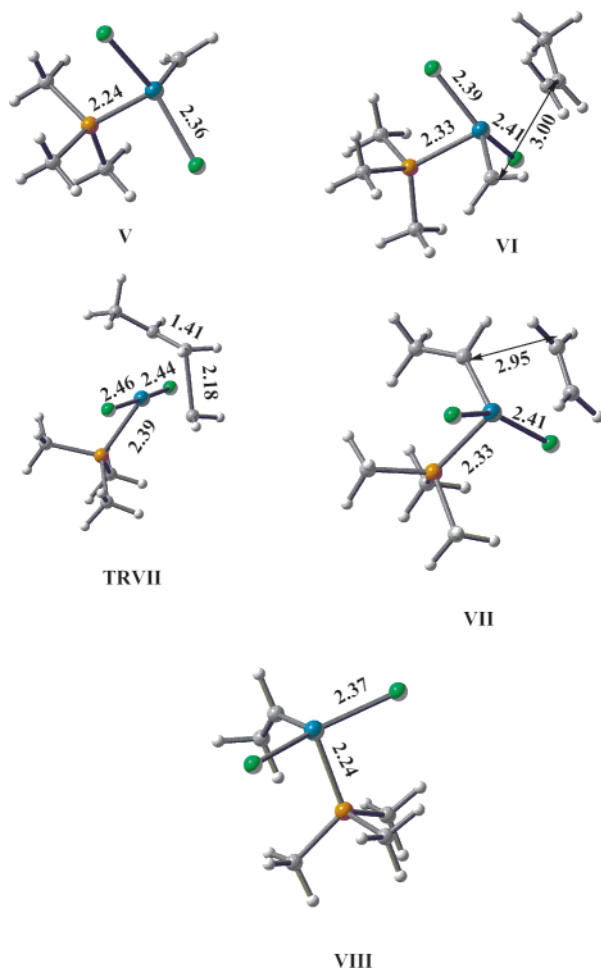


Figure 4. Equilibrium and transition state geometries of PMe_3 -containing Ru monoposphine complexes participating in the propylene metathesis reaction.

and solution, respectively. The reaction occurs with no activation energy, according to a relaxed potential energy scan carried out at the B3LYP/LACVP** level of theory. The phosphine exchange reaction in Ru diphosphine alkylidene complexes has recently been studied by Grubbs in toluene at 80 °C.¹⁴ The results show that activation enthalpies for this process lie between 27 and 19 kcal/mol, depending on complex structure, comparing favorably with dissociation energies calculated on the basis of total electronic energies (Table 2). Since no activation barrier was detected for this transformation during a relaxed potential energy search, the experimentally determined activation enthalpies correspond to the enthalpy of the phosphine exchange reaction. As can be seen, a very reasonable agreement between calculated and experimental data is observed. The loss of one phosphine molecule results in significant shortening (more than 0.1 Å) of Ru–P and Ru–Cl bonds (Figure 4), evidencing steric hindrance caused by the second phosphine molecule. A similar situation was observed in ref 18. The next step is the formation of propylene complex **VI**. Unlike complex **II** formation, this reaction is more favorable ($\Delta G = 3.5$ and 7.4 kcal/mol in the gas phase and solution, respectively), again confirming significant steric hindrance in diphosphine Ru complexes. The next step is the metathesis transformation of **VI** to **VII** occurring with free activation energies of 9.4 and 6.3 kcal/mol in the gas phase

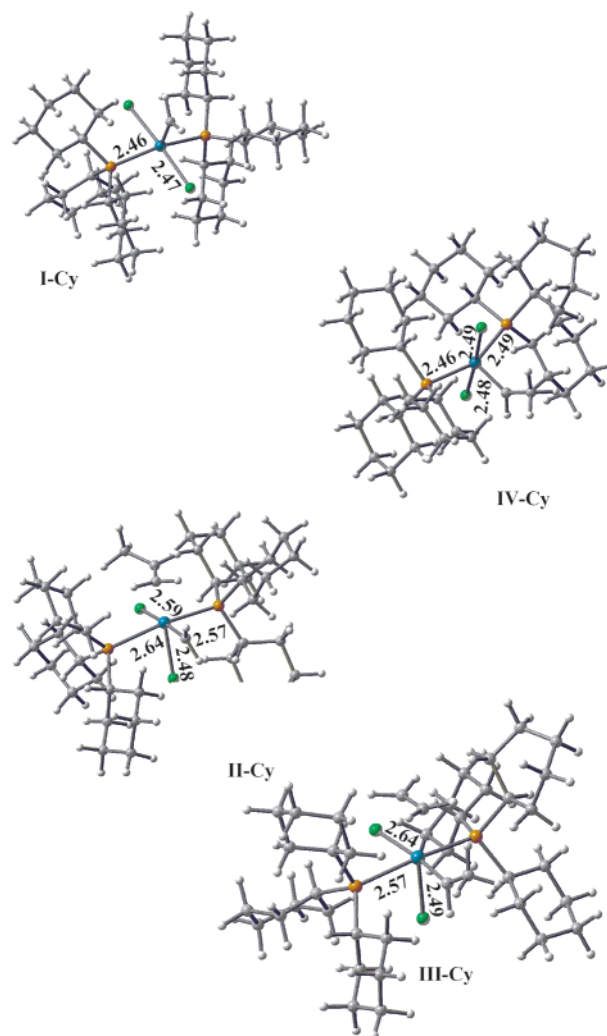


Figure 5. Equilibrium geometries of PCy_3 -containing Ru diphosphine complexes participating in the propylene metathesis reaction.

and solution, respectively. The reaction energetics are unaffected by solvent, being -0.9 kcal/mol for both the solution and gas phase. Similar to the **II**–**III** transformation, the carbene needs to rotate for the metathesis to occur (Figure 4). The decomplexation of an ethylene molecule from complex **VII** completes the metathesis transformation, forming the monoposphine complex **VIII**. This reaction is characterized by negative ΔG values of -4.9 and -8.3 kcal/mol, in the gas phase and solution, respectively. All three reaction pathways are summarized in Figure 2. As can be seen, the third pathway is much more favorable compared to the first pathway, thus excluding the second, since the second route starts with complex **II** formation similar to the first route.

It is noteworthy that when using electronic energies instead of free ones the most favorable reaction pathway is the first one (Table 2). While the electronic and free energies lead to very similar energetics (within 1 kcal/mol) for the reactions where the number of particles is constant, the entropy factor strongly favors the **I**–**V** and disfavors the **I**–**II** process, thus clearly showing the decisive role of entropy for the reaction pathway in the case of PMe_3 -containing complexes. These differences can be observed by comparing energy profiles obtained

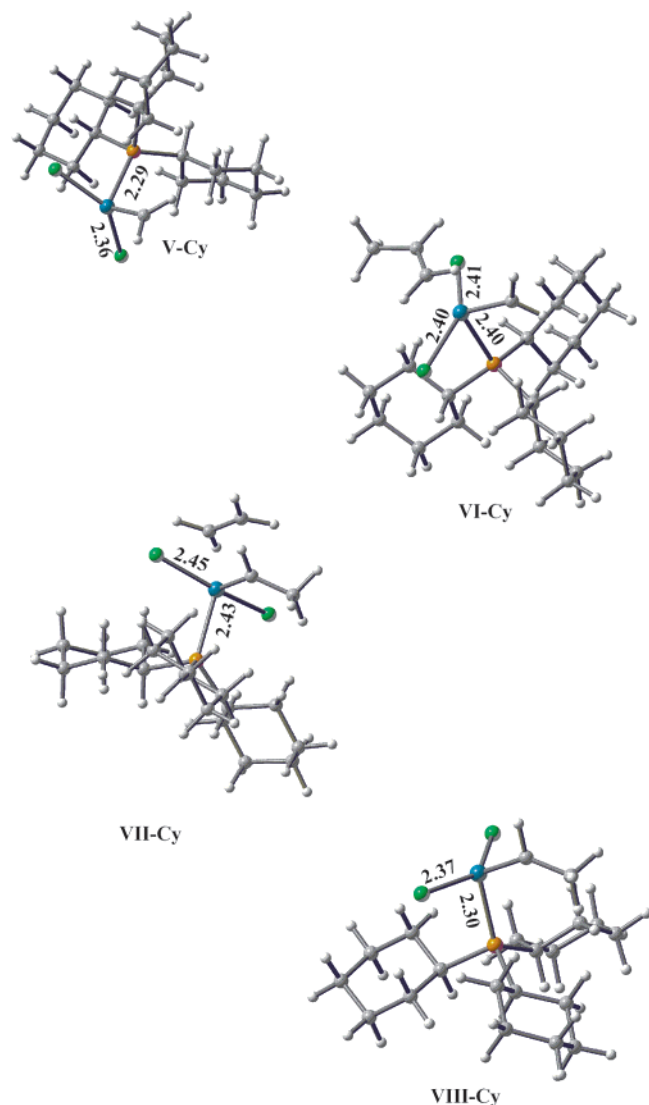


Figure 6. Equilibrium and transition state geometries of PCy_3 -containing Ru monophosphine complexes participating in the propylene metathesis reaction.

with free and total electronic energies (parts a and b of Figures 2).

The situation somewhat changes for Ru–carbene complexes containing bulky tricyclohexylphosphine ligands. Due to the very large size of optimization jobs (more than 1000 basis functions for diphosphine complexes) neither the transition state search nor the statistical mechanics calculations have been practical for PCy_3 -containing complexes. Therefore, only total electronic energies were available to discuss the reaction routes for these systems. Nevertheless, these data allow one to make clear conclusions about the reaction routes. The complexation of the diphosphine complex **I-Cy** with propylene (**I-Cy**–**II-Cy** transformation) becomes extremely unfavorable, achieving energies of 30.8 and 32.5 kcal/mol in the gas phase and solution, respectively (Table 2). If one compares ΔE and ΔG for PMe_3 -containing intermediates, it can be clearly seen that entropy factors will make the process of **II-Cy** formation even more unfavorable. As has been mentioned, the **I**–**II** process shows a free activation energy of some 23.8 kcal/mol in solution, reflected in a perceptible (0.05–0.06 Å) elongation of Ru–P bonds in complex **II**. The

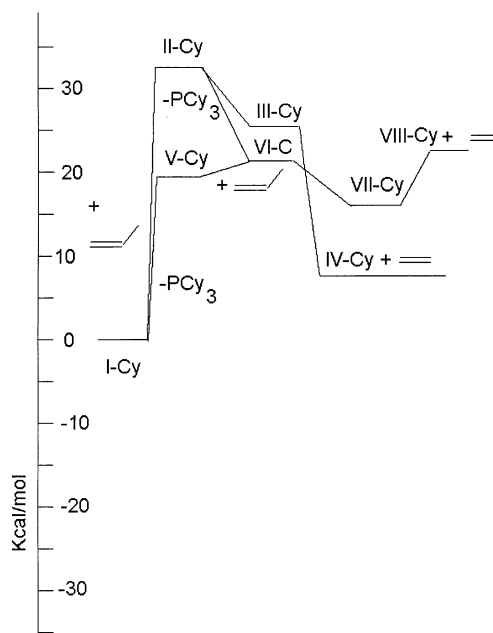


Figure 7. Total electronic energy profile for the propylene metathesis reaction mediated by a PCy_3 -containing Ru complex.

Ru–P distance increase in the **II-Cy** complex is far more significant, 0.2 Å (Figure 5), implying a higher activation energy for this process. In any case, one would expect the activation energy for **I-Cy**–**II-Cy** complexation to be similar to or higher than that of the **I**–**II** reaction, giving a value well above 50 kcal/mol. On the other hand, the elimination of one PCy_3 molecule from the diphosphine complex **I-Cy** to give the monophosphine complex **V-Cy** requires only 19.8 kcal in solution, and the Gibbs energy of this process will be more negative, as evidenced by data obtained for PMe_3 -containing molecules (Table 2), thus making this route even more favorable for bulky PCy_3 compared to the PMe_3 route. According to the calculations the Ru–P binding energy is practically independent of the alkyl moiety volume, being similar for Me and Cy groups (Table 2) and quite similar to those obtained in a recent work.¹⁸ After the monophosphine complex **V-Cy** formed, it reacted with a propylene molecule to form the weakly bonded **VI-Cy** complex (Figure 6). The metathesis reaction leads to **VII-Cy** containing ethylene, which is exothermic due to the difference in stability between primary and secondary carbenes (–1.7 and –5.3 kcal/mol in the gas phase and solution, respectively). The complex **VII-Cy** dissociates to give ethylene and the monophosphine complex **VIII-Cy**. Figures 2 and 7 summarize the reaction paths of the metathesis reaction for Ru complexes with different ligands. As can be seen from the figures, in both cases the third reaction route is more favorable compared to the first one. As can be seen from the comparison of parts a and b of Figure 2, the entropy contribution determines the reaction path for PMe_3 -containing complexes. This preference increase for the PCy_3 group is due to the fact that the formation of the complex **II-Cy** is extremely unfavorable compared to the formation of complex **II** because of steric hindrances caused by a second PCy_3 group.

Conclusions

Three different reaction pathways have been investigated for the Ru-mediated propylene metathesis reaction using the DFT approach at the B3LYP/LACVP** level. The most important conclusion that can be made from the present study is that, independent of the ligand volume, the monophosphine complex is the active catalytic species in the metathesis reaction. It has been found that for the Ru complex with PCy₃ ligands the only viable metathesis reaction mechanism is one involving elimination of one PCy₃ molecule in accordance with experimental observations. The formation of the **II-Cy** complex is extremely unfavorable in the case of the PCy₃ ligand, due to steric hindrance caused by bulky ligands forcing the elimination of one

PCy₃ molecule before the metathesis reaction can proceed.

For the smaller PMe₃ the entropy contribution is decisive for the reaction path to follow a dissociative substitution reaction path.

Acknowledgment. This investigation was supported by grants from the CONACyT (Contract Nos. 32560E and NC-204). We thank the reviewers for their very valuable comments.

Supporting Information Available: A table giving Cartesian coordinates of optimized minima and transition state structures. This material is available free of charge via the Internet at <http://pubs.acs.org>.

OM020581W